Articles

Probing Rhodopsin−Transducin Interactions by Surface Modification and Mass Spectrometry†

Xin Wang,‡ Sung-Ho Kim,‡,§ Zsolt Ablonczy,|| Rosalie K. Crouch,|| and Daniel R. Knapp*,‡

Department of Cell and Molecular Pharmacology and Experimental Therapeutics and Department of Ophthalmology, Medical University of South Carolina, Charleston, South Carolina 29425, and Department of Chemistry, Soonchunhyang University, Asan 336-745, South Korea

Received February 18, 2004; Revised Manuscript Received June 14, 2004

ABSTRACT: The interactions of rhodopsin and the α-subunit of transducin (G_t) have been mapped using a surface modification "footprinting" approach in conjunction with mass spectrometric analysis employing a synthetic peptide corresponding to C-terminal residues 340−350 of the α-subunit of G_t, $G_t\alpha$(340−350). Membrane preparations of unactivated (Rh) and light-activated rhodopsin (Rh*), each in the presence or absence of $G_t\alpha$(340−350), were acetylated with the water-soluble reagent sulfosuccinimidyl acetate, and the extent of the acetylation was determined by mass spectrometry. By comparing the differences in acetylation among Rh, Rh*, and the Rh−$G_t\alpha$(340−350) and Rh*−$G_t\alpha$(340−350) complexes, we demonstrate that the surface exposure of the acetylation sites was reduced by the conformational change associated with light activation, and that binding of $G_t\alpha$(340−350) blocks acetylation sites on cytoplasmic loops 1, 2, and 4 of Rh*. In addition, we show evidence of interaction between the end of the C-terminal tail of rhodopsin and $G_t\alpha$ in the unactivated state of rhodopsin.

Rhodopsin, the photoreceptor protein of the retinal rod cell, is a prototypical G-protein-coupled receptor (GPCR).[1] The protein contains an extracellular N-terminal tail, seven transmembrane helices, three interhelical loops on either side of the membrane, and a cytoplasmic C-terminal tail as shown in Figure 1. The chromophore, 11-*cis*-retinal, is covalently linked to a lysine residue in the transmembrane domain of the seventh helix. Upon absorption of a photon, the bound retinal is isomerized to the all-*trans* form, inducing a conformational change in the protein on the cytoplasmic side of the membrane. The conformational change leads to an active intermediate (Rh*) that binds and activates the G-protein, transducin (G_t), and initiates the visual cascade. G_t is a heterotrimeric G-protein composed of a guanine nucleotide binding α-subunit ($G_t\alpha$), and a functional complex of β- and γ-subunits ($G_t\beta\gamma$). The binding of $G_t\alpha\beta\gamma$ to Rh* catalyzes exchange of GTP with the GDP bound to $G_t\alpha$. $G_t\alpha\beta\gamma$ then dissociates from rhodopsin as the $G_t\alpha$−GTP complex and $G_t\beta\gamma$. Eventually, Rh* decays to opsin and free all-*trans*-retinal. Recently, an X-ray crystal structure showed the seven-helix bundle and intradiskal face of rhodopsin in the ground state (Rh) (*1*). However, the cytoplasmic side of the membrane, which binds and activates the G-protein, responsible for signal transduction, was not well resolved.

A variety of experimental approaches, including limited proteolysis (*2*, *3*), peptide competition (*4*), site-directed mutagenesis (*5*−*9*), and antibody binding (*10*) in combination with biochemical and biophysical assays, have been employed to map the sites of Rh and Rh* responsible for the binding and activation of G_t. The C2−C4 loops (also known as α-helix 8) on the cytoplasmic surface (Figure 1) have been found to be involved in the interaction with G_t, whereas the C-terminal tail of rhodopsin has not been reported to be involved in this interaction. A combination of site-directed mutagenesis and peptide binding showed that the amino terminus of the C4 loop interacts directly with G_t, particularly with $G_t\alpha$ (*11*, *12*). The contact sites in the Rh*−G_t complex were studied by cross-linking the S240C mutant (at the C3 loop) with G_t upon light activation (*13*, *14*). Cross-linking is reported to occur between Rh* and mainly the C-terminal Arg310−Lys313 and Glu342−Lys345 peptides and the N-terminal Leu19−Arg28 peptide of $G_t\alpha$. These results indicate that both the N- and C-termini of $G_t\alpha$ are in the proximity of the C3 loop in the Rh*−G_t complex.

† This work was supported by NIH Grants EY08239, EY14793, and EY04939 and an unrestricted grant to the Medical University of South Carolina (MUSC) from Research to Prevent Blindness, Inc. (New York, NY). R.K.C. is a RPB Senior Scientific Investigator. This work was carried out in the MUSC Mass Spectrometry Facility.

* To whom correspondence should be addressed. Telephone: (843) 792-5830. Fax: (843) 792-2475. E-mail: knappdr@musc.edu.

‡ Department of Cell and Molecular Pharmacology and Experimental Therapeutics, Medical University of South Carolina.

§ Soonchunhyang University.

|| Department of Ophthalmology, Medical University of South Carolina.

[1] Abbreviations: AspN, endoproteinase AspN; CNBr, cyanogen bromide; DM, dodecyl maltoside; ESI, electrospray ionization; GPCR, G-protein-coupled receptor; G_t, transducin; LC, liquid chromatography; MALDI, matrix-assisted laser desorption ionization; MS, mass spectrometry; MS/MS, tandem mass spectrometry; Rh, unactivated rhodopsin; Rh*, light-activated rhodopsin; SA, sulfosuccinimidyl acetate.

10.1021/bi049642f CCC: $27.50
Published on Web 08/06/2004

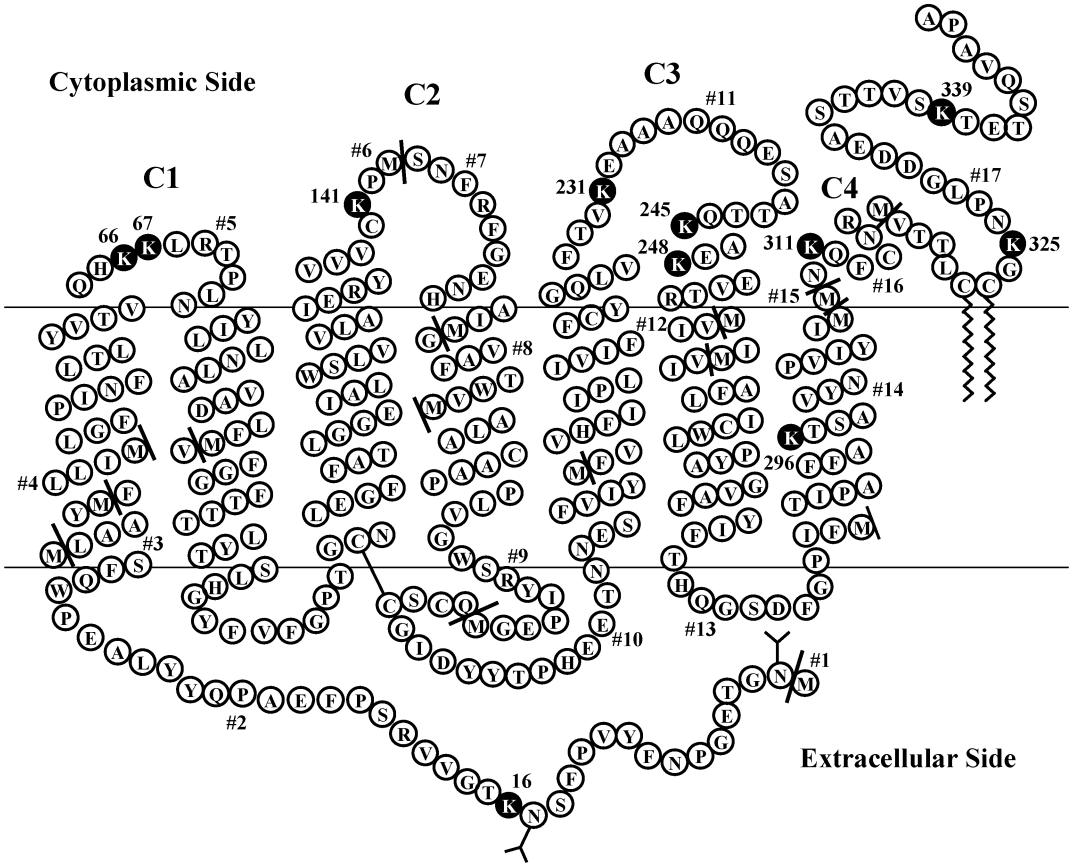

FIGURE 1: Two-dimensional model of bovine Rh with known posttranslational modifications. Lysine residues are shown as filled circles. The predicted CNBr cleavage sites are numbered. The cytoplasmic loops are labeled C1−C4. The C4 loop is also known as α-helix 8.

Both the $G_t\alpha$ (*15*, *16*) and $G_t\beta\gamma$ (*17*−*19*) subunits of the heterotrimeric complex appear to interact with Rh*. The 23 N-terminal residues and the 11 C-terminal residues of $G_t\alpha$ (*15*) and the 12 C-terminal residues of $G_t\gamma$ (*19*, *20*) are known sites of interaction. In addition, an alanine scanning mutagenesis study suggested the involvement of the $\alpha 4/\beta 6$ loop of $G_t\alpha$ (which lies adjacent to the carboxyl terminus) in the interactions with Rh* (*21*). A spectrophotometric assay, based on the stabilization of Rh* in the presence of G_t, showed that synthetic peptides $G_t\alpha(340-350)$ (*15*, *22*) and $G_t\gamma(50-71)$-farnesyl (*22*, *23*) bind and stabilize Rh*, mimicking the effect of G_t.

Of the various G_t fragments that have been reported to bind to Rh*, the C-terminal peptide of $G_t\alpha(340-350)$ (IKENLKDCGLF) has been investigated the most extensively. Hamm and colleagues (*15*) demonstrated that the $G_t\alpha(340-350)$ peptide binds to Rh* and stabilizes it. The decay of Rh* in the presence of the $G_t\alpha(340-350)$ peptide proceeds slowly, with a half-life time of 128 min, without generation of any other photoproducts of rhodopsin (*24*). Acharya and co-workers (*8*) have reported that the $G_t\alpha(340-350)$ binding site consists of residues Tyr136−Val139 in the C2 loop and residues Glu247−Thr251 in the C-terminal portion of the C3 loop.

In this paper, we report a study of the $G_t\alpha(340-350)$ peptide binding to Rh* using surface modification "footprinting" studies in conjunction with mass spectrometric analysis. Mass spectrometric analysis of integral membrane proteins has been successfully used in the mapping of bacteriorhodopsin and rhodopsin (*25*, *26*). Combined with the site-specific chemical cleavage, mass spectrometric analysis has also been used to study the intrahelical arrangement in rhodopsin (*27*). There are 10 free lysines on the surface of rhodopsin, which could potentially be modified by sulfosuccinimidyl acetate (SA). In the work reported here, the stable Rh*−$G_t\alpha(340-350)$ complex was acetylated and the relative extent of acetylation was determined by mass spectrometry (MS). The results provide evidence of the $G_t\alpha(340-350)$ peptide binding to Rh* and reveal that the C-terminal tail of Rh might also be involved in the interaction of rhodopsin with $G_t\alpha$.

EXPERIMENTAL PROCEDURES

Materials. Cyanogen bromide (CNBr, 5 mol/L in acetonitrile, Sigma-Aldrich Chemical Co., St. Louis, MO), endoproteinase AspN (AspN, Sigma), α-cyano-4-hydroxycinnamic acid (Sigma), sulfosuccinimidyl acetate (SA, Pierce Biotechnology Inc., Rockford, IL), tributylphosphine (Sigma), 4-vinylpyridine (Sigma), and dodecyl maltoside (DM, EMD Biosciences Inc., San Diego, CA) were used as received without further purification.

Rh and Peptide Preparation. Urea-washed rod outer segments were isolated from intact bovine retina (Lawson Co., Lincoln, NE) as described previously (*28*) and were stored at −80 °C under Ar in the dark. All manipulations were conducted under dim red light unless stated otherwise. $G_t\alpha(340-350)$ (IKENLKDCGLF) was synthesized by the Medical University of South Carolina Peptide Synthesis Facility and purified by LC on a C18 column (Enconosphere, Alltech Associates Inc., Deerfield, IL). The purity of the peptide was confirmed by MALDI-MS. $G_t\alpha(340-350)$ (2

mmol/L) was freshly prepared in buffer A [20 mmol/L sodium phosphate, 100 mmol/L KCl, 0.1 mmol/L EDTA, and 1.5 mmol/L DTT (pH 7.5)] and incubated at room temperature under Ar for 2−3 h before being used to ensure that the cysteines were in the reduced form.

Acetylation of Rhodopsin. Rod outer segments were resuspended in buffer A (1 μg/μL). SA (50 mmol/L) was freshly prepared in a 5 mmol/L citrate buffer (pH 5.0) prior to use. Acetylation was performed with a 50-fold molar excess of SA over total lysine residues, at a final concentration of 2 mmol/L (20 °C for 30 min), and was quenched with 15 mmol/L (final concentration) Tris buffer (pH 7.6) for 15 min. The acetylated rhodopsin was then isolated by centrifugation (88800*g* for 10 min at 4 °C), and the pellet was washed twice with H_2O. Acetylation of rhodopsin was performed under four different experimental conditions: (1) Rh in the absence of $G_t\alpha$(340−350), (2) Rh* in the absence of $G_t\alpha$(340−350), (3) Rh in the presence of $G_t\alpha$(340−350), and (4) Rh* in the presence of $G_t\alpha$(340−350). Rh* was prepared by illuminating Rh suspended in buffer with white light for 2 min using a fiber optic illuminator.

Digestions. Protein digestions were carried out as previously described with CNBr (*26*) and AspN (*29*).

LC−MS Analysis. The analysis of the CNBr-digested samples followed the methodology outlined previously (*25*, *26*) with minor modifications. The sample (~120 μg of total peptides) was loaded onto a reversed phase column (RPR-1, 100 Å, 2.1 mm × 100 mm, 5 μm particle size, Hamilton, Reno, NV). The peptides were separated using a flow rate of 400 μL/min.

The AspN-digested sample was loaded onto a reversed phase column (RPR-3, 300 Å, 1 mm × 100 mm, 10 μm particle size, Hamilton) and washed with 2% organic mobile phase for 5 min to remove salts. The gradient (flow rate of 100 μL/min) started from 2% organic mobile phase and ramped from 2 to 30% over the course of 28 min, ramped from 30 to 98% over the course of 10 min, and held at 98% for 2 min. The LC solvents were the same as with the CNBr-digested samples (*25*, *29*).

RESULTS

Identification and Relative Quantitation of the Acetylation of Lysine Residues in Rhodopsin. Figure 1 shows a two-dimensional model of bovine rhodopsin with the previously observed posttranslational modifications, the predicted CNBr cleavage sites, and potential acetylation sites. There are 11 lysine residues in bovine rhodopsin, nine of which (Lys66, -67, -141, -231, -245, -248, -311, -325, and -339) are located either in or close to the cytoplasmic side of the membrane. Lys16 is located on the extracellular side of the membrane. Lys296 is the chromophore binding site (11-*cis*-retinal is bound here via a Schiff base) and is buried in the membrane. The cytoplasmic side of the membrane binds and activates transducin in the visual transducin process. Therefore, the cleavage fragments with lysine residues located in or close to the cytoplasmic side of the membrane (CNBr fragments 5, 6, 11, 16, and 17) were investigated in detail.

The absorption spectrum of the peptide−opsin complex was measured before acetylation. No changes were found in the spectra, an indication that acetylation of the complex did not disrupt the complex (data not shown). CNBr cleavage fragments of Rh, Rh*, acetylated Rh, and acetylated Rh* were separated by LC, and their respective masses were determined by electrospray ionization MS (Table 1). A mass shift of 42 Da corresponds to the addition of one acetyl group for a singly charged fragment. Fourteen of the 17 total predicted CNBr cleavage fragments are detected in a single LC−MS run. Fragments 1 and 15 contain only a single methionine residue, and their masses are below the lower mass limit of the instrument, and thus are not detected. However, due to incomplete cleavage, fragment 14−15 and fragment 15−16 are detected. Fragment 2 has the two rhodopsin glycosylation sites (Asp2 and -15); because of the large size and heterogeneity, this fragment is not detected in our LC−MS/MS measurements, but the acetylation of lysine 16 was confirmed by MALDI-MS.

Table 1: Cyanogen Bromide Fragments of Bovine Rhodopsin[a]

fragment	residues	no. of acetylated lysines	expected mass ([M + H]$^+$)	observed mass	observed charge state	retention time (min)
1	1	0	144.1	ND[b]	−	−
2	**2−39**	**0**	**6501.8**[c]	**ND**[b]	−	−
		1	**6413.3**[c]	**ND**[b]	−	−
3	40−44	0	520.3	520	+1	23.5
4	45−49	0	588.4	588.1	+1	41.7
5	**50−86**	**0**	**4241.4**	**4240.8**	**+3**	**61.6**
		1	**4283.4**	**4282.8**	**+3**	**63.8**
		2	**4325.5**	**4323.6**	**+3**	**66.1**
6	**87−143**	**0**	**6371.3**	**6370.8**	**+4**	**67.7**
		1	**6413.3**	**6411.6**	**+4**	**69.3**
7	144−155	0	1374.7	688.0	+2	31.9
8	156−163	0	862.4	878.2[d]	+1	37.2
9	164−183	0	2177.1	2176.4	+2	40.4
10[e]	184−207	0	3005.3	3005.1	+3	35.9
11	**208−253**	**0**	**5315.8**	**5316.0**	**+3**	**61.3**
		1	**5357.8**	**5356.8**	**+3**	**62.3**
		2	**5399.9**	**5396.7**	**+3**	**63.4**
		3	**5459.9**[f]	**5456.7**[f]	**+3**	**63.5**
12	254−257	0	427.3	427	+1	26.3
13	258−288	0	3598.8	3598.0	+2	64.4
14	**289−308**	**0**	**2198.1**	**2196.6**	**+2**	**48.1**
		1	**2240.2**	**ND**[b]	−	−
15	309	0	120.1	ND[b]	−	−
14−15	**289−309**	**0**	**2329.2**	**2328.2**	**+2**	**51.0**
		1	**2371.2**	**ND**[b]	−	−
16	**310−317**	**0**	**1097.5**	**1097.8**	**+2**	**21.7**
		1	**1139.5**	**1139.0**	**+2**	**23.7**
15−16	**309−317**	**0**	**1228.6**	**1227.2**	**+2**	**23.2**
		1	**1270.6**	**1269.6**	**+2**	**25.4**
17	**318−348**	**0**	**3599.9**	**3599.7**	**+3**	**84.9**
		1	**3642.0**	**3641.7**	**+3**	**85.9**
		2	**3684.0**	**3683.4**	**+3**	**87.5**

[a] Boldface identifies fragments with acetylation sites. [b] Not detected with LC−MS. [c] Most abundant glycoform. [d] Observed with oxidized tryptophan. [e] Also observed with the N-terminal pyroglutamate form. [f] Observed with homoserine at the C-terminus.

Figure 2 shows an example of the base peak chromatogram of a CNBr-cleaved acetylated Rh* in the presence of the $G_t\alpha$(340−350) peptide with the fragments identified on the basis of MS analysis. Unlabeled peaks in Figure 2 are not rhodopsin peptides. The unacetylated, singly and doubly acetylated forms of fragments 5 and 17 are chromatographically resolved and are highly abundant, as shown in Figure 2. The increased retention times of the acetylated fragments are a consequence of the increased hydrophobicity after the acetylation of the lysines.

The quantitative analysis was based on the relative intensities of the molecular ion signals of the unacetylated and acetylated fragments detected during the LC−MS run.

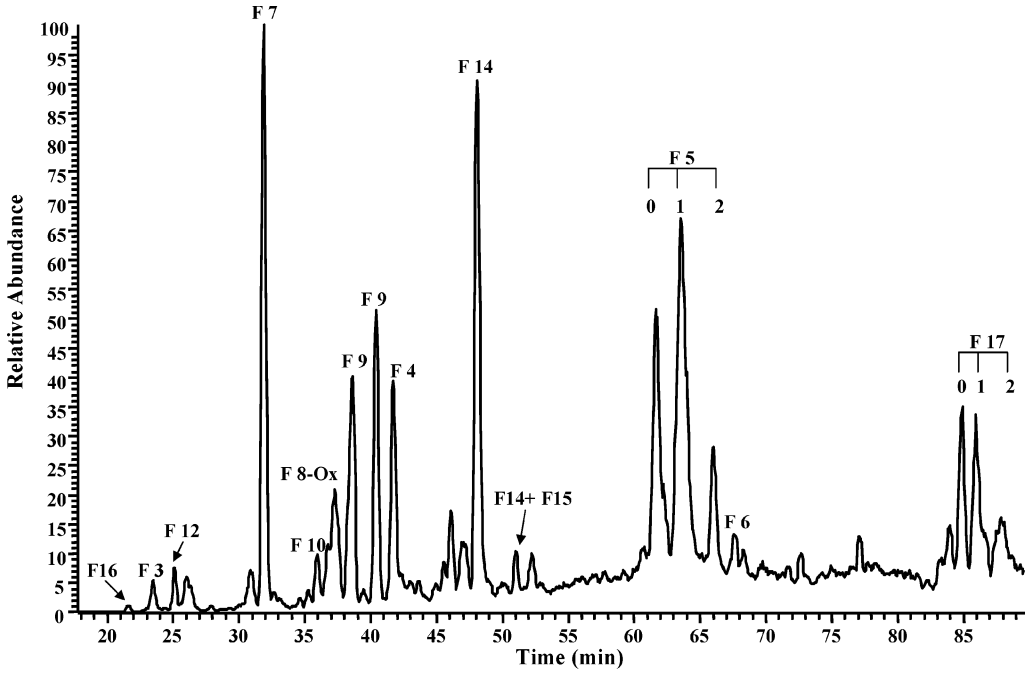

FIGURE 2: Base peak chromatogram of CNBr fragments of an acetylated Rh* in the presence of the $G_t\alpha(340-350)$ peptide. The CNBr fragments are numbered at the Met cleavage sites. Bracketed labels 0−2 represent the number of the acetylated lysine residues in CNBr fragments 5 and 17.

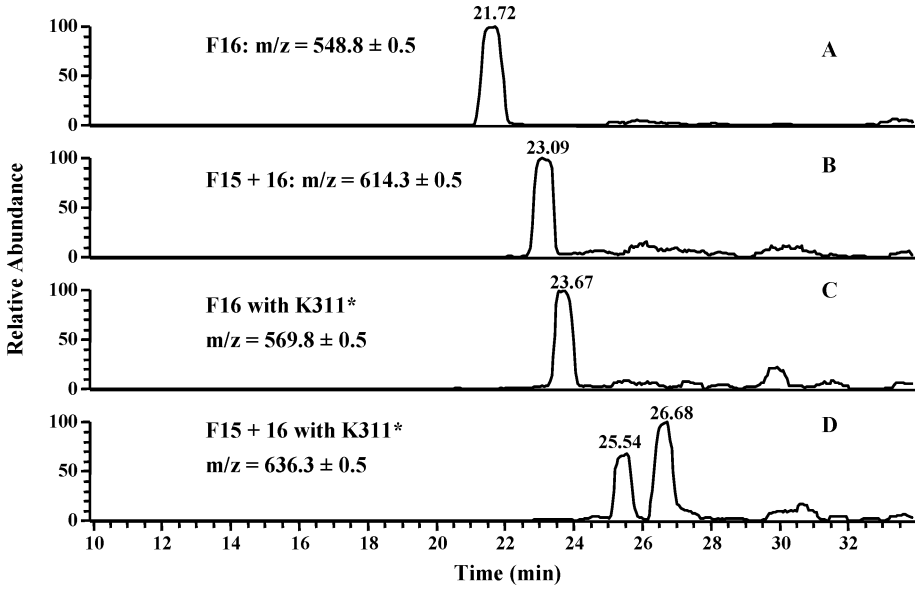

FIGURE 3: Reconstructed ion chromatograms of CNBr fragment 16. Panels A and B represent the reconstructed ion chromatograms of unacetylated CNBr fragment 16 and incompletely cleaved fragment 15−16, respectively. Panels C and D represent the reconstructed ion chromatograms of acetylated CNBr fragment 16 and incompletely cleaved fragment 15−16, respectively.

By specifying the predicted molecular ions, we reconstructed selected ion chromatograms and calculated the relative peak areas using Xcalibur. Figure 3 shows one example of the reconstructed ion chromatograms of the unacetylated (A) and the acetylated (C) CNBr fragment 16, and the unacetylated (B) and the acetylated (D) CNBr fragment 15−16 (from incomplete CNBr cleavage at Met314). An average mass shift of 21 Da was observed for the doubly charged acetylated fragment in both cases.

The identities of the peaks were further confirmed by MS/MS spectra as shown in Figure 4. Most of the b ions, y ions, and the loss of vinylpyridine (in the y ion series) were detected. A mass shift of 42 Da was observed in the b ion series (b_2*−b_7*) in acetylated fragment 16. There are two peaks at *m*/*z* 636.3 ± 0.5 Da in the ion chromatogram of acetylated fragment 15−16 (Figure 3D). After the MS/MS spectra for both peaks had been analyzed, only the first peak at 25.54 min was identified as acetylated fragment 15−16. The second peak did not appear to be a peptide and thus was excluded from the quantitation analysis. The relative amount of the acetylated fragment was calculated from the relative peak area of the acetylated fragment compared to the sum of the total peak areas of the acetylated and unacetylated fragments, assuming that the unacetylated and acetylated peptides have similar ionization efficiencies. In the case of incomplete cleavages, the total peak area includes those of the incompletely cleaved unacetylated and acetylated fragments as well.

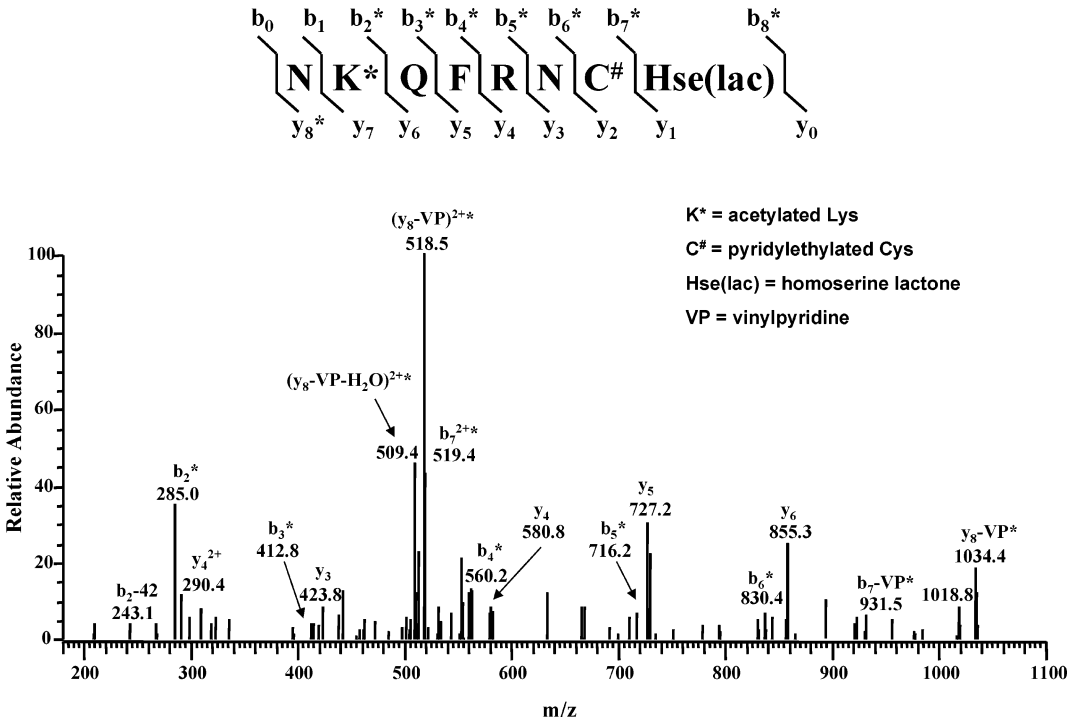

FIGURE 4: MS/MS spectrum of acetylated CNBr fragment 16.

Table 2: Normalized (percentage) Acetylations under Different Experimental Conditions

CNBr fragment	acetylated residues	no peptide (no. of experiments)		peptide (no. of experiments)	
		Rh	Rh*	Rh	Rh*
5	K66 or K67 (C1 loop)	100	107.4 ± 6.5[a] (8)	97.4 ± 6.5[a] (8)	92.6 ± 4.9 (8)
	K66 and K67 (C1 loop)	100	79.3 ± 8.2 (8)	100.2 ± 9.4[a] (8)	24.5 ± 2.2 (8)
6	K141 (C2 loop)	100	81.2 ± 7.5 (8)	97.7 ± 7.0[a] (8)	62.8 ± 6.9 (7)
16	K311 (C4 loop)	100	94.9 ± 10.2[a] (8)	110.2 ± 12.1[a] (8)	46.4 ± 5.7 (8)
17	K325 (C-terminus)	100	50.3 ± 9.2[b] (4)	123.3 ± 9.3 (4)	64.2 ± 8.9[b] (4)
	K339 (C-terminus)	100	99.8 ± 0.4[a] (4)	23.8 ± 3.8[c] (4)	34.0 ± 3.1[c] (4)

[a] There is no significant difference when compared with the value for Rh without peptide ($P > 0.05$). [b] There is no significant difference between these two values ($P > 0.05$). [c] There is no significant difference between these two values ($P > 0.05$).

Acetylation of the Cytoplasmic Surface of Rhodopsin. Figure 5 summarizes the acetylation of the cytoplasmic surface of rhodopsin under the four different experimental conditions. Panels A−D show the percentages of the acetylated CNBr fragments 5, 6, 16, and 17, respectively. For CNBr fragments 5 (Figure 5A) and 17 (Figure 5D) which have two lysine residues, "singly acetylated" represents the percentage of the fragment with only one lysine residue acetylated while "doubly acetylated" represents the percentage of the fragment with both lysine residues acetylated. The sum of the percentages of the acetylated and unacetylated fragments (which are not indicated in the figures) always equals 100%. To separate the effects of light and transducin binding on the acetylation of lysine residues, Rh and Rh* were acetylated in the presence and absence of the $G_t\alpha(340-350)$ transducin mimic peptide. Light exposure and the presence of the $G_t\alpha(340-350)$ peptide selectively influenced the acetylation of each lysine residue. For a more convenient comparison, Table 2 shows the data normalized to the percentage of the respective peptide of Rh when $G_t\alpha(340-350)$ was not present (the solid dark columns in Figure 5).

*$G_t\alpha(340-350)$ Blocks the Acetylation of the C1 Loop in Rh**. CNBr fragment 5 (Leu50−Met86) contains Lys66 and -67 located in the C1 loop of rhodopsin. As seen in Figure 5A, the presence or absence of $G_t\alpha(340-350)$ has no effect on the acetylation of these lysine residues in the Rh state, as the normalized percentages are the same within the experimental error (Table 2, columns 1 and 2), showing that Rh is indifferent to the peptide. However, light activation changes this situation. In the Rh* state, the level of single acetylation is reduced by 14% and the level of double acetylation decreases by 69% in the presence of $G_t\alpha(340-350)$ (Table 2, columns 3 and 4). This result indicates that binding of the transducin mimic peptide in a manner that blocks acetylation of one of these lysines is promoted by the rhodopsin structural changes after light activation. Interestingly, light activation alone (without the peptide) implies a major conformational change in the C1 loop, as the level of double acetylation decreased by 21% in Rh* compared to that in Rh. This, on the other hand, means the reduction in the accessibility of one of the lysine residues by the rhodopsin structural changes following light activation. Therefore, the light-induced binding of $G_t\alpha$ to the C1 loop coincides with a structural rearrangement which hides some part of the loop from the surface. Further investigation is needed to determine why only one of the lysine residues is mainly affected, which one of the neighboring residues becomes less accessible in light, and which one of these residues has a role in the interaction of Rh* with transducin.

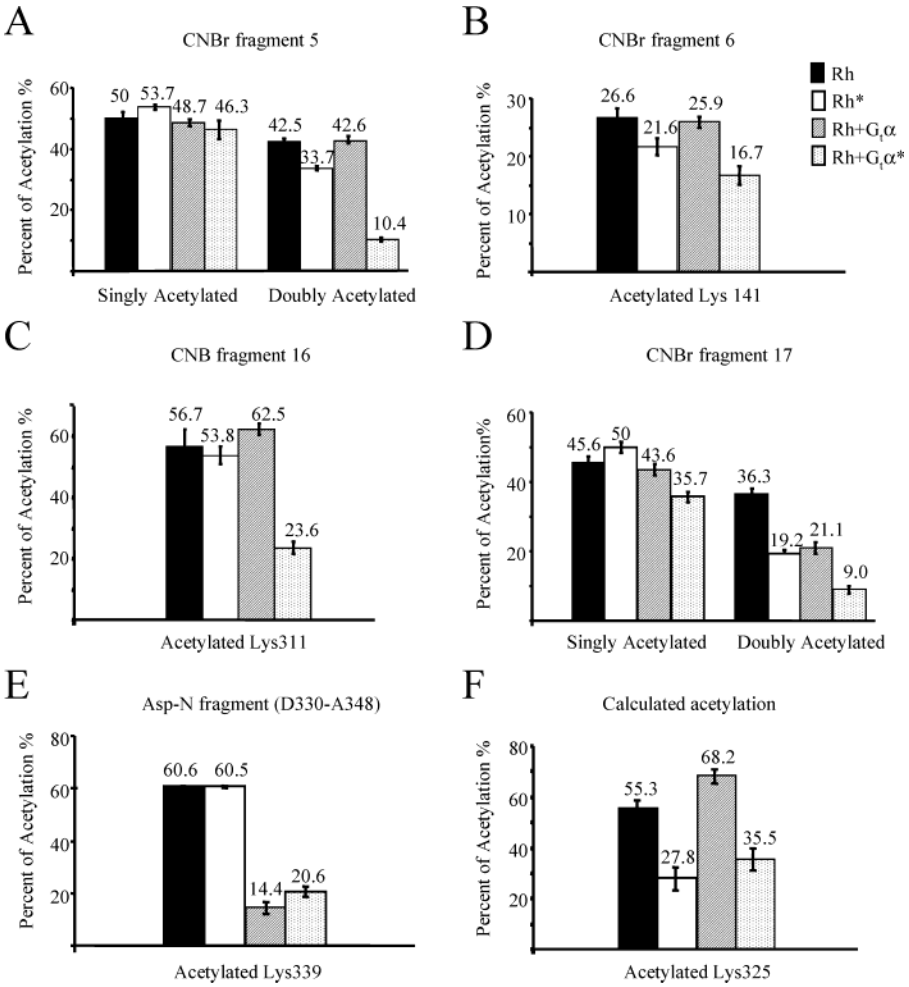

FIGURE 5: Results of acetylation of Rh under four experimental conditions. Panels A−D depict the percentage of acetylated CNBr fragments 5, 6, 16, and 17, respectively. In panels A and D, "Singly Acetylated" represents the percentage of the fragment with only one lysine residue acetylated and "Doubly Acetylated" represents the percentage of the fragment with two lysine residues acetylated. Panel E depicts the percentage of the acetylated C-terminal fragment after AspN digestion (Asp330−Ala348). Panel F depicts the calculated percent acetylation of Lys325. In all panels, bars 1 (black) and 2 (white) represent the acetylation of unactivated (Rh) and light-activated (Rh*) rhodopsin, respectively, in the absence of the $G_t\alpha$(340−350) peptide. Bars 3 (dark gray) and 4 (light gray) represent the acetylation of Rh and Rh*, respectively, in the presence of the $G_t\alpha$(340−350) peptide. Each bar represents the mean percentage of acetylation ± standard error. The bars are labeled with the actual mean values. See Table 2 for the number of experiments.

*$G_t\alpha$(340−350) Blocks the Acetylation of the C2 Loop in Rh**. CNBr fragment 6 (Val87−Met143) contains Lys141 that is located in the C2 loop of rhodopsin. Figure 5B indicates that only 27% of fragment 6 is acetylated, which is lower than the acetylation level in any other fragments. The hydrophobic residues (^{137}VVVC^{140}) near Lys141 may inhibit the accessibility of the water-soluble acetylation reagent. The overall behavior of Lys141 is similar to that of the lysines of fragment 5, but the binding of the transducin peptide is less dramatic. In the Rh state, the presence or absence of $G_t\alpha$(340−350) does not make a significant difference, but after light activation, the acetylation of Lys141 decreased by 23% when the peptide was present. There was also a similar light-only effect as the level of acetylation of Lys141 was reduced by 19% in Rh* when compared to that in Rh without $G_t\alpha$(340−350). These results suggest that while the light-induced structural changes decrease the level of exposure of the C2 loop and Lys141 similarly, or slightly more than the level of the C1 loop, they are much less affected by the binding of the $G_t\alpha$ peptide.

*$G_t\alpha$(340−350) Blocks the Acetylation of the C4 Loop in Rh**. CNBr fragment 16 (Asp310−Met317) contains Lys311 that is located in the C4 loop of rhodopsin. As seen in Figure 5C, in contrast to CNBr fragments 5 and 6, neither the $G_t\alpha$-(340−350) peptide in the Rh state nor light activation alone affects the acetylation of Lys311. However, there was a 51% decrease in the level of acetylation following light activation when the $G_t\alpha$(340−350) peptide was present. These data suggest clear light-induced binding of the $G_t\alpha$ peptide in a manner that blocks the C4 loop of rhodopsin, indicating that the region of the C4 loop has a less dynamic role, but it is significantly affected by transducin binding to Rh*.

*$G_t\alpha$(340−350) Blocks the Acetylation of the C-Terminal Tail of Rh and Rh**. CNBr fragment 17 (Val318−Ala348) contains Lys325 and -339 on the C-terminal tail of rhodopsin. The behavior of the acetylation of CNBr fragment 17 was unique in the sense that this was the only fragment where binding of $G_t\alpha$(340−350) to Rh reduced the accessibility of a lysine residue to acetylation. As shown in Figure 5D, there was a 42% decrease in the level of double acetylation of the fragment even in the Rh state when the transducin peptide was added, while in the other regions of the protein, only light-induced peptide binding effects could be observed. Light activation appears to promote further binding, since

in Rh*, the level of single acetylation was reduced by 29% and the level of double acetylation by 53% after the addition of the peptide. Another interesting feature of the acetylation of the C-terminal tail was the large 48% reduction in the level of double acetylation invoked by light only, without the peptide. These results show a predominant effect of light-induced structural rearrangement causing less surface exposure, but the role of this region in the binding of the mimic peptide is not significantly affected by light exposure. The fact that the peptide binding halves the level of acetylation in both Rh and Rh* implies that the roles of the two lysine sites might be distinct.

*$G_t\alpha$(340−350) Binds to Lys339 in both Rh and Rh**. To determine how each lysine residue in the C-terminal tail of rhodopsin is affected by light and the peptide, endoproteinase AspN was used to cleave the acetylated rhodopsin, as the AspN digest peptide (Asp330−Ala348) contains only Lys339. As seen in Figure 5E and Table 2, the acetylation of Lys339 was found to be unaffected by light either with or without the peptide, but the peptide reduces the level of acetylation by 76% in Rh and 66% in Rh*. These results suggest that the end of the C-terminal tail in Rh may be involved in the binding of $G_t\alpha$, but that this portion of rhodopsin is not significantly affected by any light-induced structural changes.

*$G_t\alpha$(340−350) Promotes the Acetylation of Lys325 in both Rh and Rh**. The measurement of the level of acetylation of CNBr fragment 17 (containing both Lys325 and Lys339) and of the AspN fragment (containing only Lys339) allows calculation of the extent of acetylation of Lys325. The measured acetylated AspN fragments, the total acetylated Lys339 (S_{339}), represent a mixture of two states of acetylated CNBr fragment 17: one with both Lys325 and Lys339 acetylated (the measured doubly acetylated CNBr fragment 17 (D_{CNBr17}) and another from the portion of singly acetylated CNBr fragment 17 (S_{CNBr17}) where only Lys339 was acetylated (not measured; designated for calculations as *a*):

$$S_{339} = D_{CNBr17} + a \quad (1)$$

Similarly, the percentage of the total acetylated Lys325 (S_{325}) is a mixture of the measured percentage of doubly acetylated CNBr fragment 17 and the portion of the singly acetylated CNBr fragment 17 where only Lys325 was acetylated (not measured; designated as *b*):

$$S_{325} = D_{CNBr17} + b \quad (2)$$

Adding these quantities and taking into account that $S_{CNBr17} = a + b$:

$$S_{339} + S_{325} = 2D_{CNBr17} + S_{CNBr17}(1 + 2)$$

Thus

$$S_{325} = 2D_{CNBr17} + S_{CNBr17} - S_{339} \quad (3)$$

Since D_{CNBr17}, S_{CNBr17}, and S_{339} were measured, the percentage of the acetylated Lys325 can be calculated from eq 3, the results of which are shown in Figure 5F and Table 2. Interestingly, the percentage of acetylated Lys325 increased 23% in the Rh state, but was not significantly changed in the Rh* state in the presence of the peptide. On the other hand, the percentage of the acetylated Lys325 decreased after light activation by 50% without the peptide and by 48% with the peptide. These results suggest that the presence of the peptide induced some conformational change that leads to an increased level of exposure of Lys325, and that light activation decreases the level of exposure of Lys325 regardless of the presence of $G_t\alpha$(340−350). The very different behavior of Lys325 and Lys339 indicates that in contrast to its more distal region, the portion of the C-terminal rhodopsin tail proximal to the palmitoyl membrane anchor does undergo light-activated structural rearrangement, but it does not directly take part in transducin binding. Rather, the binding of transducin might induce some reorganization resulting in a more exposed C-terminus.

Acetylation of the C3 Loop Is Inconclusive. CNBr fragment 11 (Phe208−Met253) contains Lys231, -245, and -248, which are located on the C3 loop. Although this loop is part of the cytoplasmic surface, the fragment is not included in the quantitative analysis presented in Figure 5 and Table 2. Even prior to acetylation, the observed signal for this fragment is very low. After acetylation, the analysis is further complicated by the partitioning of the already low signal among unacetylated and singly, doubly, and triply acetylated forms. Moreover, these peptides eluted close to the acetylated forms of CNBr fragment 5 and also to CNBr fragment 13 under our LC gradient, as shown in Table 1, causing further reduction of the signals for fragment 11 peptides due to competitive effects. MALDI-MS analysis of the collected LC fractions confirmed the presence of singly, doubly, and triply acetylated forms of fragment 11 (data not shown), suggesting that the lysine residues are exposed and accessible to the acetylation reagent. However, complete quantitative information could not be obtained, even though the collected fraction was subjected to secondary enzymatic digestion and LC−MS analysis.

DISCUSSION

Rhodopsin undergoes conformational changes upon light activation, which allow binding of transducin on the cytoplasmic surface. Modification of lysine has been used previously as a tool to study rhodopsin. Barclay and Findlay (*30*) showed the lysines could be succinylated in the dark without affecting the spectral properties of rhodopsin. Longstaff and colleagues (*31*) reported that eight or nine residues of rhodopsin could be acetylated in the dark without interfering with rhodopsin regeneration or G-protein activation. The goal of this study was to probe the interaction of rhodopsin and the $G_t\alpha$(340−350) peptide using surface modification and MS analysis. There are two factors that influence the acetylation of the lysine residues in the protein: light exposure and binding of the $G_t\alpha$(340−350) peptide. Figure 6 presents a three-dimensional model of the cytoplasmic surface of rhodopsin showing the lysines whose acetylation was affected by binding of the $G_t\alpha$(340−350) peptide.

Light-Induced Conformational Changes. Recently, Khorana, Hubbell, and co-workers (*32*−*35*) proposed conformational changes of rhodopsin in a micellar solution upon light activation based on site-directed spin labeling studies. In their model, upon light activation, the helical bundle opens up at its cytoplasmic end, exposing various regions for interactions with transducin. The proposed changes include outward movements of the cytoplasmic ends of helices 2, 3, 6, and

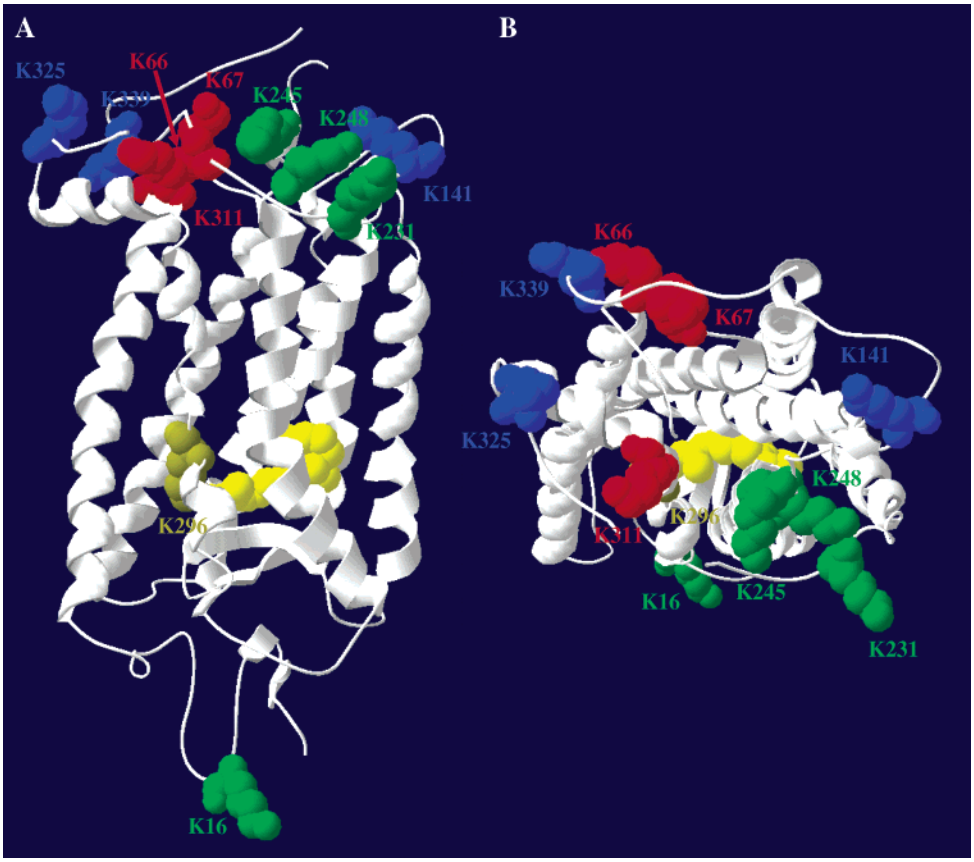

FIGURE 6: (A) Side view and (B) top view of lysines in rhodopsin. The 11-*cis*-retinal bound to Lys296 is yellow, while the binding site itself is identified with a dark yellow color. Acetylation of the green colored residues was detected but not quantified. The lysines that exhibit the most prominent light-induced decrease in the level of acetylation after the addition of Gtα(340−350) are red, while blue identifies the ones that exhibit a smaller difference. The lysines exhibiting more interaction with the peptide are found in a confined space of the cytoplasmic surface. The three-dimensional model was prepared with the DeepView/Swiss-PdbViewer, using chain A of entry 1L9H from the Protein Data bank.

7. Only a small movement between helix 4 and the C4 loop was observed (*35*). Additional evidence for the movement of the C-terminal segment of helix 7 away from the core of the protein is provided by the fact that residues 304−311 (a peptide segment of helix 7 near the C4 loop) are only accessible to an antibody after light activation (*10*) (for a recent review, see ref *36*).

Another structural model for Rh* derived from solution NMR of peptides (*37*) also predicts that a crevice opens in a groove between the C2 and C3 loops on the cytoplasmic domain of Rh*. Some residues in the C1 loop form the floor of the groove. The conformational change upon light activation prepares a surface for transducin binding that is partially occluded in Rh. These investigators suggest that the entire groove on the cytoplasmic face of Rh* may be involved in binding transducin.

Our results confirm and extend these previous observations. Upon light activation, the level of acetylation of the lysine residues located in the C1 and C2 loops and the amino terminus of the C-terminal tail is decreased, suggesting that the C1 and C2 loops and the C-terminal tail undergo conformational changes that lead to a reduced level of exposure of these lysine residues. The changes upon light activation in the acetylation of Lys66, -67, and -141 located in the C1 and C2 loops are relatively small. As shown in the crystal structure and spin labeling studies (*1*, *38*, *39*), these residues are relatively exposed and easily accessible, which may account for the small change in their exposure upon light activation. In addition, very small or no changes were found in and around residues 60−66 and in residues 137, 141, 151, 152, 154, and 155 between Rh and Rh*, based on spin labeling (*38*, *39*).

Although residues 304−311 are reported to be accessible to antibody after light activation (*10*), we did not observe any light-induced changes in the C4 loop. High-resolution solution ^{19}F NMR spectra of fluorine-labeled rhodopsin mutants showed little or no chemical shift changes at positions 245 and 311 upon light activation, suggesting that residues 245 and 311 face the outside of the helical bundle and are easily accessible (*40*). Residue 311 is reported to be highly mobile, accessible, and modestly reactive based on site-directed spin labeling (*41*). In addition, only a slight relative movement between helix 1 and the C4 loop was observed (*35*). Our results support these observations.

The level of acetylation of Lys325 decreased dramatically upon light activation (Table 2), suggesting that a relatively large conformational change at the C-terminal tail adjacent to the palmitoylation sites reduces the level of exposure of Lys325. However, the acetylation of Lys339 does not change after light activation, suggesting that the accessibility of Lys339 is not affected. Previous spin labeling studies (*42*) showed that the C-terminal tail beyond residue 328 is highly disordered and similar to an unfolded protein. This area is also not resolved in the crystal structure (*1*). There is no steric restraint at the extreme of the C-terminal tail, so the accessibility of the acetylation

reagent is not limited by the conformational change upon light activation. On the other hand, the sequence of residues 325−328 has a stable configuration (*42*), and it folds back and packs against the C4 loop in the crystal structure (*1*). In addition, Lys325 is adjacent to the palmitoylation sites, which may restrict its accessibility.

Light-Induced $G_t\alpha$(340−350) Binding. Via a comparison of the differences in acetylation between Rh* and the Rh*−$G_t\alpha$(340−350) complex, our data suggest that, after light activation, the $G_t\alpha$(340−350) peptide blocks the acetylation of lysine residues located in the C1, C2, and C4 loops. The light-induced conformational changes at the C1 and C2 loops and the beginning of the C-terminal tail expose the binding domain, and then the peptide binds and blocks the exposure of mainly the C1 and C4 loops, and to a lesser extent the C2 loop, as shown by the reduced level of acetylation. This suggests that the C1 and C4 loops may be the main regions involved in the interaction with G_t. However, it must be pointed out that our studies were carried out with a short peptide, and until the studies are conducted with the full protein, these results are only suggestive.

The role of the C1 loop in the interaction with G_t is not clear from previous studies. A peptide competition study showed that the synthetic peptide corresponding to residues 61−75 in the C1 loop is not an effective competitor for binding of G_t, suggesting it is not involved in the interaction with G_t (*4*). In addition, alanine mutants T62A/V63A/Q64A, K66A/K67A, L68A/R69A/T70A, and P71A were found to have G_t activity similar to that of the wild-type protein (*43*). However, cysteine mutants K66C, K67C, L68C, and P71C exhibited a 50−70% decrease in the level of G_t activation when compared with that of the wild type (*38*). A longer peptide corresponding to residues 64−84 in the C1 loop has been shown to inhibit the signal transduction cascade more effectively than the shorter peptide (corresponding to residues 60−75 in the C1 loop), suggesting that the C1 loop may be involved in the binding of G_t (*37*). Our results show that the $G_t\alpha$(340−350) peptide blocks the acetylation of Lys66 and Lys67 on light activation, again indicating that the C1 loop may be involved.

The lack of light-induced C-terminal $G_t\alpha$(340−350) binding supports results by other researchers proposing that the C-terminal tail is not involved in the activation of G_t (*2*−*4*, *9*, *11*, *12*, *37*). A synthetic peptide corresponding to residues 323−348 in the C-terminal tail of Rh failed to compete with the Rh* for binding of G_t (*4*). A C-terminal truncation mutant (C316stop) binds and activates G_t normally, suggesting that amino acids Cys316−Ala348 are not necessary for the activation of G_t (*9*). Because of the lack of light-induced C-terminal $G_t\alpha$(340−350) binding, our data support these conclusions. However, an interesting finding in our study is that the $G_t\alpha$(340−350) peptide blocks the acetylation of Lys339 in Rh and no additional interaction was found between the extreme of the C-terminal tail and the peptide by light activation. These data indicate peptide binding, also reinforced by the increased level of acetylation of Lys325 observed under the same conditions, which suggests that the binding around Lys339 increases the level of exposure of Lys325 and thus affects the whole tail. NMR spectroscopy studies showed that an analogue peptide, $G_t\alpha$(340−350)-K341R, binds to both Rh and Rh* (*44*), but the native $G_t\alpha$-(340−350) peptide binds to only Rh* and not to Rh (*24*). Our results suggest that the extremity of the C-terminal tail might be a site of interaction of Rh with G_t. There is no difference in the acetylation of Lys325 between Rh* and Rh when the peptide is present, suggesting that the peptide definitely does not bind the C-terminal tail region adjacent to the palmitoylation sites after light activation. The role of the interaction between the C-terminal tail and the peptide in Rh is not clear. A possibility is that the C-terminus serves as a recognition site for G_t binding and activation or that the C-terminus prevents interaction of G_t with other cytoplasmic loops before rhodopsin is activated.

In summary, we have applied a footprinting approach that combines surface modification and MS in the analysis of the interaction between rhodopsin and the $G_t\alpha$(340−350) peptide. This work demonstrates the change in the level of exposure of the lysine residues located in the cytoplasmic loops of rhodopsin upon light activation and the interaction of the $G_t\alpha$(340−350) peptide with the cytoplasmic loops in the Rh*. In addition, the experiments provide evidence of interaction between the end of the C-terminal tail of unactivated rhodopsin and G_t. These results support the current model of G-protein binding and activation by GPCRs.

ACKNOWLEDGMENT

We thank Dr. Mas Kono for helpful discussions and Ms. Lauren Magaldi for editorial assistance.

NOTE ADDED AFTER ASAP POSTING

This article posted to the ASAP website on August 6, 2004 contained two errors. The last sentence before the Results should have been deleted and the Rh* term was incorrect on line 568. This information has been corrected in this new version posted August 10, 2004.

REFERENCES

1. Palczewski, K., et al. (2000) Crystal struture of rhodopsin: A G-protein coupled receptor, *Science 289*, 739−745.
2. Kuhn, H., and Hargrave, P. A. (1981) Light-induced binding of guanosine triphosphatase to bovine photoreceptor membranes: Effect of limited proteolysis of the membranes, *Biochemistry 20*, 2410−2417.
3. Wehner, M., and Kuhn, H. (1987) The cyclic GMP enzyme cascade of vision: Site of light activation localized by enzymatic modifications of rhodopsin, *Adv. Biosci. 62*, 345−351.
4. Konig, B., et al. (1989) Three cytoplamic loops of rhodopsin interact with transducin, *Proc. Natl. Acad. Sci. U.S.A. 86*, 6878−6882.
5. Franke, R. H., et al. (1988) A single amino acid substitution in rhodopsin (Lys248-Leu) prevents activation of transducin, *J. Biol. Chem. 263*, 2119−2122.
6. Yang, K., et al. (1996) Structure and function in rhodopsin. Single cysteine substitution mutants in the cytoplasmic interhelical E−F loop region show position-specific effects in transducin activation, *Biochemistry 35*, 12464−12469.
7. Ridge, K., et al. (1995) Structure and function in rhodopsin. Separation and characterization of the correctly folded and misfolded opsins produced on expression of an opsin mutant gene containing only the native intradiscal cysteine codons, *Biochemistry 34*, 3261−3267.
8. Acharya, S., Saad, Y., and Karnik, S. S. (1997) Transducin: a C-termial peptide binding site consists of C−D and E−F loops of rhodopsin, *J. Biol. Chem. 272*, 6519−6524.
9. Weiss, E. R., et al. (1994) Effects of carboxyl-terminal truncation on the stability and G-protein coupling activity of bovine rhodopsin, *Biochemistry 33*, 7587−7593.

10. Abdulaev, N. G., and Ridge, K. D. (1998) Light-induced exposure of the cytoplasmic end of transmembrane helix seven in rhodopsin, *Proc. Natl. Acad. Sci. U.S.A. 95*, 12854−12859.
11. Marin, E. P., et al. (2000) The amino terminus of the 4th cytoplamic loop of Rh modulated Rh-transducin interaction, *J. Biol. Chem. 275*, 1930−1936.
12. Ernst, O. P., et al. (2000) Mutation of the 4th cytoplasmic loop of Rh affects binding of transducin and peptides derived from the C-terminal sequences of transducin α subunits, *J. Biol. Chem. 275*, 1937−1943.
13. Cai, K., Itoh, Y., and Khorana, H. G. (2001) Mapping of contact sites in complex formation between transducin and light-activated Rh by covalent crosslinking: Use of a photoactivable reagent, *Proc. Natl. Acad. Sci. U.S.A. 98*, 4877−4882.
14. Itoh, Y., Cai, K., and Khorana, H. G. (2001) Mapping of contact sites in complex formation between light-activated Rh and transducin by covalent crosslinking: Use of a chemically preactivated reagent, *Proc. Natl. Acad. Sci. U.S.A. 98*, 4883−4887.
15. Hamm, H. E., et al. (1988) Site of G protein binding to Rh mapped with synthetic peptides from the α subunit, *Science 241*, 832−835.
16. Hamm, H. E., et al. (1987) Mechanism of action of monoclonal antibodies that block the light activation of the guanyl nucleotide-binding protein, transducin, *J. Biol. Chem. 262*, 10831−10838.
17. Kelleher, D. J., and Johnson, G. L. (1988) Transducin inhibition of light-dependent rhodopsin phosphorylation: evidence for $\beta-\gamma$ subunit interaction with rhodopsin, *Mol. Pharmacol. 34*, 452−460.
18. Phillips, W. J., and Cerione, R. A. (1992) Rhodopsin/transducin interactions. I. Characterization of the binding of the transducin-$\beta\gamma$ subunit complex to rhodopsin using fluorescence spectroscopy, *J. Biol. Chem. 267*, 17032−17039.
19. Kisselev, O., Ermolaeva, M., and Gautam, N. (1995) Efficient interaction with a receptor requires a specific type of prenyl group on the G protein γ subunit, *J. Biol. Chem. 270*, 25356−25358.
20. Kisselev, O., et al. (1995) Receptor-G protein coupling is established by a potential conformational switch in the $\beta\gamma$ complex, *Proc. Natl. Acad. Sci. U.S.A. 92*, 9102−9106.
21. Natochin, M., et al. (1999) Roles of the transducin α-subunit, a 4-helix/β6 loop in the receptor and effector interactions, *J. Biol. Chem. 274*, 7865−7869.
22. Kisselev, O., et al. (1999) Signal transfer from Rh to the G-protein: Evidence for a two-site sequential fit mechanism, *Proc. Natl. Acad. Sci. U.S.A. 96*, 4898−4903.
23. Kisselev, O., Ermolaeva, M., and Gautam, N. (1994) A farnesylated domain in the G protein γ subunit is a specific determinant of receptor coupling, *J. Biol. Chem. 269*, 21399−21402.
24. Kisselev, O., et al. (1998) Light-activated Rh induces structural binding motif in G protein a subunit, *Proc. Natl. Acad. Sci. U.S.A. 95*, 4270−4275.
25. Ball, L. E., et al. (1998) Mass spectrometric analysis of intergral membrane proteins: Application to complete mapping of bacteriorhodopsins and rhodopsin, *Protein Sci. 7*, 758−764.
26. Ablonczy, A., et al. (2001) Mass spectrometric analysis of integral membrane proteins at the subnanomolar level: application to recombinant photopigments, *Anal. Chem. 73*, 4774−4779.
27. Gelasco, A., Crouch, R. K., and Knapp, D. R. (2001) Intrahelical arrangement in the integral membrane protein rhodopsin investigated by site-specifice chemical cleavage and mass spectrometry, *Biochemistry 39*, 4907−4914.
28. McDowell, J. H., and Kuhn, H. (1977) Light-induced phosphorylation of rhodopsin in cattle photoreceptor membranes: Substrate activation and inactivation, *Biochemistry 16*, 4054−4060.
29. Ablonczy, Z., et al. (2002) 11-*cis*-Retinal reduces constitutive opsin phosphorylation and improves quantum catch in retinoid deficient mouse rod photoreceptors, *J. Biol. Chem. 277*, 40491−40498.
30. Barclay, P. L., and Findlay, J. B. (1984) Labelling of the cytoplasmic domains of ovine rhodopsin with hydrophilic chemical probes, *Biochem. J. 220*, 75−84.
31. Longstaff, C., Calhoon, R. D., and Rando, R. R. (1986) Chemical modification of rhodopsin and its effect on regeneration and G protein activation, *Biochemistry 25*, 6311−6319.
32. Altenbach, C., et al. (1996) Structural features and light-dependent changes in the cytoplasmic interhelical E−F loop region of rhodopsin: A site-directed spin-labeling study, *Biochemistry 35*, 12470−12478.
33. Farrens, D. L., et al. (1996) Requirement of rigid-body motion of transmembrane helices for light activation of rhodopsin, *Science 274*, 768−770.
34. Altenbach, C., et al. (2001) Structure and function in rhodopsin: mapping light-dependent changes in distance between residue 316 in helix 8 and residues in the sequence 60−75, covering the cytoplasmic end of helices TM1 and TM2 and their connection loop CL1, *Biochemistry 40*, 15493−15500.
35. Altenbach, C., et al. (2001) Structure and function in rhodopsin: mapping light-dependent changes in distance between residue 65 in helix TM1 and residues in the sequence 306−319 at the cytoplasmic end of helix TM7 and in helix H8, *Biochemistry 40*, 15483−15492.
36. Hubbell, W. L., et al. (2003) Rhodopsin structure, dynamics, and activation: a perspective from crystallography, site-directed spin labeling, sulfhydryl reactivity, and disulfide cross-linking, *Adv. Protein Chem. 63*, 243−290.
37. Choi, G., et al. (2002) Structural studies of metarhodopsin II, the activated form of the G-protein coupled receptor, rhodopsin, *Biochemistry 41*, 7318−7324.
38. Klein-Seetharaman, J., et al. (1999) Single-cysteine substitution mutants at amino acid positions 55−75, the sequence connecting the cytoplasmic ends of helices I and II in rhodopsin: reactivity of the sulfhydryl groups and their derivatives identifies a tertiary structure that changes upon light activation, *Biochemistry 38*, 7938−7944.
39. Farahbakhsh, Z. T., et al. (1995) Mapping light-dependent structural changes in the cytoplasmic loop connecting helices C and D in rhodopsin: a site-directed spin labeling study, *Biochemistry 34*, 8812−8819.
40. Klein-Seetharaman, J., et al. (1999) NMR spectroscopy in studies of light-induced structural changes in mammalian rhodopsin: Applicability of solution ^{19}F NMR, *Proc. Natl. Acad. Sci. U.S.A. 96*, 13744−13749.
41. Altenbach, C., et al. (1999) Structural features and light-dependent changes in the sequence 306−322 extending from helix VII to the palmitoylation sites in rhodopsin: A site-directed spin-labeling study, *Biochemistry 38*, 7931−7937.
42. Langen, R., et al. (1999) Structural features of the C-terminal domain of bovine rhodopsin: A site-directed spin-labeling study, *Biochemistry 38*, 7918−7924.
43. Shi, W., et al. (1995) Rhodopsin mutants discriminate sites important for the activation of rhodopsin kinase and Gt, *J. Biol. Chem. 270*, 2112−2119.
44. Dratz, E. A., et al. (1993) NMR structure of a receptor-bound G-protein peptide, *Nature 263*, 276−281.

BI049642F